INTERFACE

royalsocietypublishing.org/journal/rsif

Research

Cite this article: Conway JM, Meily P, Li JZ, Perelson AS. 2021 Unified model of short- and long-term HIV viral rebound for clinical trial planning. *J. R. Soc. Interface* **18**: 20201015. https://doi.org/10.1098/rsif.2020.1015

Received: 14 December 2020
Accepted: 23 March 2021

Subject Category:
Life Sciences–Mathematics interface

Subject Areas:
biomathematics

Keywords:
HIV, viral rebound, latency, mathematical modelling

Author for correspondence:
Jessica M. Conway
e-mail: jmconway@psu.edu

†Present address: University of Illinois College of Veterinary Medicine, Urbana, IL, USA.

Electronic supplementary material is available online at https://doi.org/10.6084/m9.figshare.c.5361991.

THE ROYAL SOCIETY PUBLISHING

Unified model of short- and long-term HIV viral rebound for clinical trial planning

Jessica M. Conway[1], Paige Meily[2,†], Jonathan Z. Li[3] and Alan S. Perelson[4]

[1]Department of Mathematics and Center for Infectious Disease Dynamics, Pennsylvania State University, University Park, PA, USA
[2]University of Pennsylvania School of Arts and Sciences, Philadephia, PA, USA
[3]Brigham and Women's Hospital, Harvard Medical School, Boston, MA, USA
[4]Theoretical Biology and Biophysics, Los Alamos National Laboratory, Los Alamos, NM, USA

JMC, 0000-0003-1474-4230

Antiretroviral therapy (ART) effectively controls HIV infection, suppressing HIV viral loads. Typically suspension of therapy is rapidly followed by rebound of viral loads to high, pre-therapy levels. Indeed, a recent study showed that approximately 90% of treatment interruption study participants show viral rebound within at most a few months of therapy suspension, but the remaining 10%, showed viral rebound some months, or years, after ART suspension. Some may even never rebound. We investigate and compare branching process models aimed at gaining insight into these viral dynamics. Specifically, we provide a theory that explains both short- and long-term viral rebounds, and post-treatment control, via a multitype branching process with time-inhomogeneous rates, validated with data from Li *et al*. (Li *et al*. 2016 *AIDS* **30**, 343–353. (doi:10.1097/QAD.0000000000000953)). We discuss the associated biological interpretation and implications of our best-fit model. To test the effectiveness of an experimental intervention in delaying or preventing rebound, the standard practice is to suspend therapy and monitor the study participants for rebound. We close with a discussion of an important application of our modelling in the design of such clinical trials.

1. Introduction

With the advent of antiretroviral therapy (ART), the prospects of people living with HIV (PLWH) improved immeasurably, with ART improving both the quality and length of life [1,2]. However ART is not a cure; while regular dosing with ART does effectively control the infection and hold the amount of circulating virus below the level detectable by clinical assays, suspension of therapy is typically followed by HIV rebound to high viral loads [3].

Recent results give significant nuance to 'typical' viral rebound following analytic treatment interruption (ATI). In a 2013 prospective study, a cohort of 14 PLWH (the VISCONTI cohort) were identified, who were able to control HIV infection for a prolonged period—upwards of a decade—after stopping ART [4]. Results from the VISCONTI study and others suggest that post-treatment controllers (PTCs) may control HIV using a mechanism distinct from that of spontaneous HIV controllers [5,6]. Li *et al*. identified a distinct cohort of PTCs, who maintained viral loads less than or equal to 400 HIV RNA copies ml^{-1} for greater than or equal to 24 weeks [7,8], in a pooled analysis of participants from AIDS Clinical Trials Group (ACTG) studies, the Montreal Primary HIV Infection cohort, the Seattle Primary Infection Program, and the Ragon HIV Controllers cohort. Since ART comes with a number of drawbacks including side-effects and cost, the search for biological indicators (biomarkers) of lasting ART-free HIV remission has become a priority in HIV cure research [9,10], with some good progress made [11–15].

Another significant priority is to find treatments and treatment strategies that may induce ART-free remission or even HIV cure [16,17]. Recently, two promising strategies were described, employing latency-reversing agents and immune system modulators [18,19].

When investigating the efficacy of interventions intending to delay or prevent rebound, the standard is stop therapy and observe whether rebound occurs via regular viral load tests. However, there is significant heterogeneity in HIV viral dynamics following ATI: in a pooled analysis of outcomes from six ACTG ATI studies, Li *et al.* reported widely varying times to viral rebound, with a significant number of participants maintaining viral suppression to undetectable levels for up to two or more months in the absence of ART [12]. A good characterization of such dynamics would be of significant use in demonstrating efficacy of interventions that may delay rebound.

An obvious toolset would be survival analysis, which is used to analyse the expected duration of time until one or more events—in this case, duration until viral rebound. However viral rebound dynamics are not well predicted by standard stylized survival distributions, e.g. the Weibull or the lognormal distribution, as we show in the Results (§3.1, figure 2). More specifically, they reasonably predict short-term viral rebounds, within a few months, but fail to describe delayed viral rebound that occurs after many months or years. To make up for this deficit, we derive a mechanistically motivated survival function that more accurately describes both short- and long-term viral rebound.

Within-host modelling of HIV infection is a well-established field [20–29]. Much of our quantitative understanding of HIV dynamics within a host, e.g. the infected cell death rate, the rate of viral clearance, and the number of progeny virions released from an infected cell, i.e. the burst size, derive from models fit to data [30–32]. Existing models have mainly focused on the kinetics of early infection and the effects of treatment. But recent years have seen the development of models of HIV post-treatment control [28] and the time to viral rebound after treatment cessation. Hill *et al.* [33,34] provided estimates of viral rebound time distributions, used in combination with careful and thoughtful consideration of within-host parameters, to evaluate the needed efficacy of therapeutic agents that might one day yield HIV cure. First estimates of HIV recrudescence rates were provided by Pinkevych *et al.* [35,36]. Fennessey *et al.* investigated SIV viral rebound in macaques infected with barcoded virus, to generate more detailed insights into viral rebound [37]. Building on these insights, we integrated biomarkers, specifically an individual's levels of cell-associated HIV RNA (HIV CA-RNA) and ART regimen pre-analytic treatment interruption (ATI) [12,38], into a stochastic model to start to move towards personalized viral rebound time predictions [39]. Working towards more personalization, Bing *et al.* [40] recently demonstrated that both empirical and mechanistic modelling approaches with post-ATI viral load data identify the same predictors of viral rebound, giving modelling support to identification of rebound delay predictors including pre-ATI ART regimen [12,38,39], time of initiation of ART [12] and higher nadir CD4+ T-cell counts [40]. And in a different vein, Wu *et al.* used the barcoded virus data from [37] to investigate the impact of hypothesized fluctuations in activation rates over time [41]. Notably, these models have mainly emphasized viral rebound over short timescales, in part because rebound datasets are small and therefore seldom include data on rare long-term viral rebounds. In this present study, we use data from Li *et al.*'s pooled analysis of six ATI studies [12], with 235 total study participants, large enough to begin to characterize both short-term rebound and long-term rebound simultaneously.

As with previous models, we rely primarily on the hypothesis that viral rebound is driven by latent cell activation [28,33–36,39,40]. However, the latent reservoir is heterogeneous, with recent studies suggesting it is composed of clones with different antigen specificity [42,43] and different integration sites [44], factors that can influence the propensity of latently infected cells to reactivate and produce replication competent virus. Further there are indications that immune responses play a role in determining rebound times, with studies suggesting that significantly delayed rebounds may be associated with additional mechanisms of infection control, such as anti-HIV immune responses [28], and T-cell exhaustion markers are predictive of a shorter time to viral rebound [15]. To model the impact that this heterogeneity may have on latent cell activation inducing viral rebound, we will investigate models of latent cell activation that are heterogeneous in time, which serves as a contrast to most previous studies [35,36,39,40,45] which assumed constant latent cell activation rates, with Wu *et al.* [41] being an exception. Thus, we aim to capture both short- and long-term viral rebound.

In the following, we will investigate models of viral rebound that offer improved survival distributions, i.e. a cumulative probability density function for the probability of an individual's viral rebound at time t. Armed with an effective simple model we will discuss the biological insight offered by parameter estimates obtained by fitting the model to data. In particular, we show that one can derive from our model the number of patients in an ATI clinical trial needed to detect an intervention-associated viral rebound delay relative to baseline.

2. Methods

2.1. Description of data

The description of the data we employ and associated collection methodologies are fully explained in [12]. Briefly, participants in six ACTG ATI studies (ACTG 371 [46], A5024 [47], A5068 [48], A5170 [49], A5187 [50] and A5197 [51]) were included if they were on suppressive ART, received no immunologic interventions (e.g. therapeutic vaccination, interleukin-2), and had HIV-1 RNA less than 50 copies ml^{-1} at the time of ATI ($N = 235$ participants). Early after treatment interruption, most studies reported weekly viral load measurements, with the exception of A5170 for which the median interval between viral load measurements was 5 days within six weeks ATI, though the interquartile range is broad, from 2 to 20 days. Viral rebound was defined as sustained viral loads of at least 200 HIV RNA copies ml^{-1}.

In a previous study [39], we restricted our analysis to the subset of participants that had peripheral blood mononuclear cells (PBMCs) and plasma available for HIV reservoir quantification while on ART prior to the ATI, that had CA-RNA above the level of detection at ATI, and who showed viral rebound less than or equal to 60 days after ART cessation ($N = 84$ participants). However, here we aim to develop a mechanistically motivated, phenomenological model that describes both short- and long-term viral rebound in all patients that undergo ATI and analyse data from all $N = 235$ study participants.

Finally, we acknowledge that defining viral rebound is challenging when examining data from real study participants. We define viral rebound as having occurred following a first viral

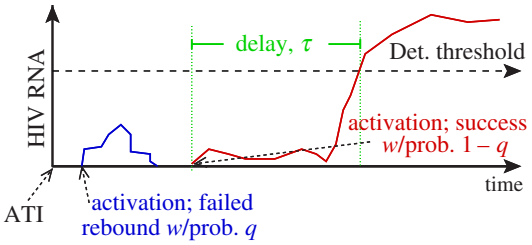

Figure 1. Model schematic [39]. Following ATI, we assume that latent cell activations are followed by chains of infection that successfully re-establish high viral loads associated with chronic infection, with probability $1-q$, or die out, with probability q. We assume further a delay τ between a successful activation and the time when plasma viraemia is detectable.

load measurement above 50 copies ml^{-1} given all subsequent viral load tests show detectable viraemia, ideally above 200 copies ml^{-1}. Some judgement was applied in cases where those conditions were not met (e.g. study participant 14 594, see electronic supplementary material figure S2). Viral dynamics for all study participants under consideration are provided in electronic supplementary material figure S2, with the last undetectable/first detectable viral load measurements we employ for our parameter estimation marked in blue and red, respectively.

2.2. Model

Our baseline model was described in [39]. In brief, as in previous studies we assume that activation of latently infected cells drives viral rebound [28,34,35,39]. We envision ensuing dynamics as illustrated in figure 1. We do not assume that all latently infected cell activations cause viral rebound. Rather, we assume that activation is followed by rounds of viral replication, which may cause viral populations to grow to detectable levels, thereby causing viral rebound, or to die out. We define q as the probability of 'die out', i.e. that the activation of a latently infected cell does not cause viral rebound. Then $1-q$ is the probability of a 'successful latent cell activation', which does cause viral rebound. Finally, we assume that there is a delay between successful latent cell activation and detectable infection, where 'detectable infection' corresponds to the study participant's viral loads exceeding 50 HIV RNA copies ml^{-1}. For simplicity, we take a fixed, delta-distributed delay; in a previous study [39], we found that, while a Weibull distribution best described the delay, per the Akaike information criterion (AIC), the improvement over other stylized distributions, including a fixed delay, was not statistically significant [39].

Taking the latent reservoir size at the time of ATI and later to be L_0, and assuming that the latently infected cells are activated at *per capita* rate a, infected cell influx occurs at the constant rate aL_0. Then the recrudescence (successful activation) rate is $r=(1-q)aL_0$. Because the latent reservoir has a half-life of approximately 44 months [52,53], and our dataset extends only about 2 years post-ATI, assuming a constant latent reservoir may introduce little error. Nonetheless, later we relax this assumption.

From a mathematical standpoint, we employ a branching process framework to construct from these assumptions a probability of viral rebound at time t. Given the recrudescence rate $r=aL_0(1-q)$, from a simple branching (immigration) process formulation we can compute the cumulative probability of successful activation at time t, $P_{\mathrm{ACT}}(t)=1-\exp\left(-(1-q)aL_0t\right)$ (see [39] for derivation). Then, assuming a fixed delay τ, i.e. delta-distributed delay $\delta(t-\tau)$, the probability of viral rebound by time t predicted by our model is

$$P_{\mathrm{VR}}(t)=\begin{cases}0, & 0\le t<\tau\\ 1-\mathrm{e}^{-(1-q)aL_0(t-\tau)}, & t\ge\tau\end{cases} \tag{2.1}$$

(see again [39]). We call this is the baseline model; below we will also investigate alternate, time-inhomogeneous, formulations for the recrudescence rates and derive the associated $P_{\mathrm{VR}}(t)$. We will use these to derive likelihood functions,

$$\mathrm{lik}(\boldsymbol{\theta})=\prod_{i=1}^{235}\left(P_{\mathrm{VR}}(t^{(i)}_{\mathrm{first}};\boldsymbol{\theta})-P_{\mathrm{VR}}(t^{(i)}_{\mathrm{last}};\boldsymbol{\theta})\right), \tag{2.2}$$

where $P_{\mathrm{VR}}(t)$ is the cumulative probability of viral rebound, multiplied over the 235 study participants, $\boldsymbol{\theta}$ are the parameters, and $t^{(i)}_{\mathrm{first}}$ and $t^{(i)}_{\mathrm{last}}$ are the times of the first detectable and last undetectable viral load measurements, respectively, for the ith study participant. Note that in using this likelihood function equation (2.2), we do not estimate viral rebound times from the data, e.g. by the mid-time point between the last undetectable and first detectable viral load measurement, in advance of the analysis. We therefore avoid the subtle uncertainty such pre-processing can create, particularly as we aim to use data that includes study participants with viral load measurements that are months apart. For all models, we estimate parameters using maximum-likelihood methods, and compare model fits using the AIC [54]. Thus, we test how well the models explain observations of viral rebound [12].

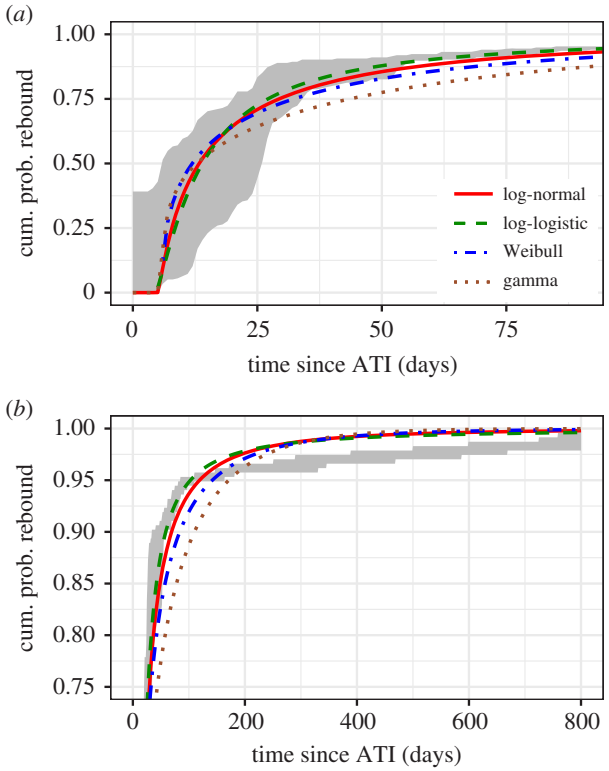

Figure 2. Typical survival curve distributions fit to viral rebound data [12], shown over (*a*) short timescales and (*b*) long timescales. The shaded region bounds the empirical distributions for the times of last undetectable and first detectable viral load tests across all study participants. To fit the distribution parameters, we define a likelihood $\mathrm{lik}(\boldsymbol{\theta})=\prod_{i=1}^{235}\left(P_{\mathrm{VR}}(t^{(i)}_{\mathrm{first}};\boldsymbol{\theta})-P_{\mathrm{VR}}(t^{(i)}_{\mathrm{last}};\boldsymbol{\theta})\right)$ where $P_{\mathrm{VR}}(t)$ is the cumulative distribution (log-normal, log-logistic or Weibull), with parameters $\boldsymbol{\theta}$, and $t^{(i)}_{\mathrm{last}}$ and $t^{(i)}_{\mathrm{first}}$ correspond to the last undetectable and first detectable viral load, respectively, for study participant i, summed over 235 study participants for whom we have data [12]. To maximize the likelihood, we employed the Davidon–Fletcher–Powell optimization algorithm implemented by the Bhat package in R [55]. The data are described in §2.1.

3. Results

We begin by providing a motivating result, showing that viral rebound dynamics are not well predicted by standard stylized survival distributions, e.g. the Weibull or the lognormal

distribution, as alluded to in the Introduction (§1). This observation provided the impetus for us to derive our mechanistically based viral rebound time distribution.

We document our first effort, estimating model parameters for the baseline model, equation (2.1), and show that this simple model does not improve predictions of long-term viral rebound relative to the standard survival distributions. We then discuss and justify alternate hypotheses for recrudescence, showing that a recrudescence rate which decreases with time explains the data much better. Finally, we discuss how our model predictions can be used to inform clinical trial design.

3.1. Viral rebound dynamics are not well predicted by standard stylized survival distributions

Survival analysis provides a natural toolset to analyse time-to-event data such as the HIV viral rebound data that forms the focus of this present study. However, when fitting the data to standard stylized survival distributions, i.e. Weibull, lognormal, log-logistic or gamma distributions, we find that viral rebound dynamics are not well predicted by these models. While the log-logistic distribution gives the best fit per the AIC (see electronic supplementary material, table S1), visual inspection of the fits in figure 2 suggests that while they reasonably predict short-term rebound, within a few months of ATI, they fail to describe delayed viral rebounds occurring after many months or years. To estimate parameters for the survival distributions, we use the likelihood function in equation (2.2) with the cumulative density function of the desired distribution as P_{VR}. To maximize the likelihood, we employed the Davidon–Fletcher–Powell optimization algorithm implemented by the Bhat package in R [55].

What follows is a derivation and justification of our mechanistically motivated survival function that more accurately describes both short- and long-term viral rebound to make up for the deficit presented by stylized distributions. Since the log-logistic distribution explains the data best, in the following it will be used as a comparator to quantify the improvements that our model brings.

3.2. Constant r fails to explain both short- and long-term rebound

We start by fitting the baseline model, equation (2.1), to the data, using maximum likelihood methods. Specifically we use the Davidon–Fletcher–Powell optimization algorithm to estimate model parameters, the recrudescence rate $r = a(1-q)L_0$ and the delay τ. Note that we cannot fit a or q individually because, with the infectious latent reservoir size L_0, they form a non-identifiable parameter combination. A summary of these parameter estimates for the baseline model are provided in table 1 and the best fit of the model to the data is shown in figure 3. Note that we found that the data for long times was too sparse to characterize a delay, so to estimate the delay τ we used an estimate derived by fitting the model only to rebounds within 60 days.

Assuming a constant recrudescence rate explains short-term viral rebound data reasonably well (figure 3*a*). However, even a visual inspection shows that the model only poorly explains both short- and long-term viral rebound data simultaneously (figure 3*b*). This is borne out in comparisons of AIC, which shows poor performance relative to most survival distributions (i.e. it increases the AIC such that $\Delta\text{AIC} > 250$ for best-fit,

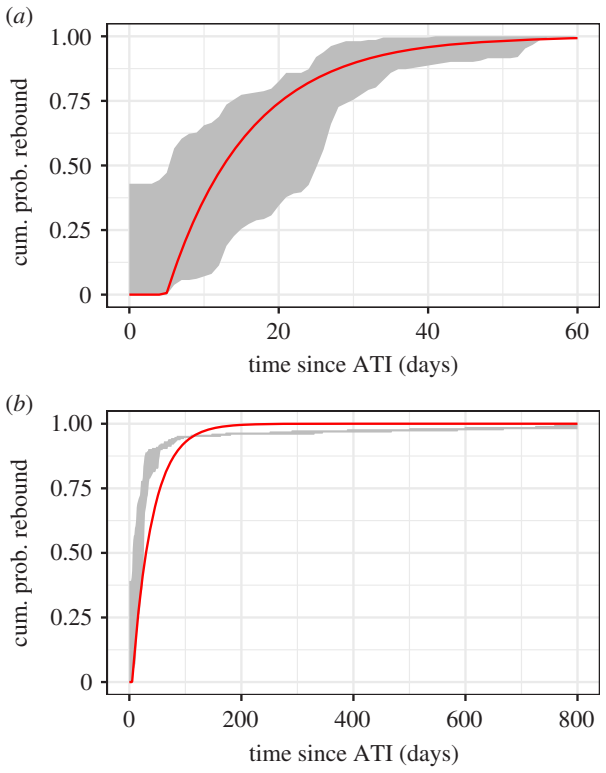

Figure 3. Baseline, constant recrudescence rate model, equation (2.1), fit to viral rebound data (see §2.1), with parameters estimates for data on (*a*) short timescales, less than or equal to 60 days only, and (*b*) short and long timescales, up to 800 days of observations. The shaded region bounds the empirical distributions for the times of last undetectable and first detectable viral load tests across all study participants.

log-logistic distribution), though it does offer an improvement on the worst-fit gamma-distribution assumption ($\Delta\text{AIC} \approx 4$) (electronic supplementary material, table S1). Thus while our model assuming a constant recrudescence rate does explain short-term viral rebound (see also [39]) it does not explain both short- and long-term viral rebound, nor does it offer any improvement over standard survival analysis distributions.

3.3. Exponentially decaying $a(t)$ explains both short- and long-term viral rebound

The failure of our baseline model, which assumes a constant recrudescence rate, is not really a surprise. For one, it relies on the assumption of a constant replication-competent latent reservoir size, and studies have shown that the latent reservoir size usually decays over time in the presence of effective therapy [52,53]. Presumably, the reservoir would similarly continue to decay post-ATI but pre-rebound, since the viral load remaining undetectable implies that robust viral replication, which may replenish the reservoir, is unlikely. Further, we recently showed that short-term viral rebounds are actually better explained by multiple successful latent cell activations in succession, with detectable viraemia composed of virus arising from replication in multiple lineages [56]. Lastly and importantly, we completely neglected the inherent heterogeneity of the latent reservoir. Post-ATI viral rebound can occur in PLWH with markers indicating small viral reservoirs [12,57,58], suggesting reservoir characteristics beyond size are associated with rebound. The latent reservoir is composed primarily of memory cells [59], each of which may be specific for a pathogen or set of pathogens. Recent characterization suggests that the

Table 1. Parameter estimates for the baseline model equation (2.1), assuming a constant recrudescence rate r. ΔAIC is computed relative to the best stylized distribution, the log-logistic, see electronic supplementary material, table S1. Note that when estimating the recrudescence rate from all the data, we used the delay τ estimated using data restricted to rebounds less than 60 days from ATI.

time window	parameters	estimates (95% CI)	ΔAIC
rebound within 60 days of ATI	$r = (1-q)aL_0$	0.0902 (0.0771,0.1054) per day	n.a. (restricted data)
	delay τ	4.93 (4.24,5.70) days	
rebound across all observed times	$r = (1-q)aL_0$	0.0278 (0.0231,0.0335) per day	252.6 (with one parameter)
	delay τ	4.93 days fixed	

Table 2. Parameter estimates for viral rebound models assuming different time-dependent recrudescence rates. ΔAIC is computed relative to the best-fit stylized distribution, the log-logistic, with parameter estimates in electronic supplementary material, table S1.

	recrudescence rate ($r(t)$) model	parameters	estimate (95% CI)	ΔAIC
(1)	$r(t) = r_0\, e^{-k(t-\tau)}$	r_0	0.058 (0.049,0.069) per day	77.7
	single-phase decay, with	k	0.011 (0.009,0.014) per day	
	$r(t) \to 0$ as $t \to \infty$	τ	4.04 (3.28,4.94) days	
(2)	$r(t) = r_\infty + (r_0 - r_\infty)e^{-k(t-\tau)}$	r_0	0.088 (0.073,0.106) per day	−10.7
	single-phase decay, with	r_∞	0.002 (0.001, 0.004) per day	
	$r(t) \to r_\infty \neq 0$ as $t \to \infty$	k	0.029 (0.022,0.040) per day	
		τ	4.98 (4.58,5.41) days	
(3)	$r(t) = r_\infty\, e^{-k_2(t-\tau)} + (r_0 - r_\infty)\, e^{-k_1(t-\tau)}$,	r_0	0.088 (0.068,0.113) per day	−8.7
	where $k_2 < k_1$	r_∞	0.002 (0.001,0.004) per day	
	biphasic decay, with	k_1	0.029 (0.019,0.053) per day	
	$r(t) \to 0$ as $t \to \infty$	k_2	$5 \times e^{-07}$ ($1 \times e^{-10}$, 0.002) per day	
		τ	4.98 (4.57,5.42) days	

reservoir is largely made up of clonal populations [60–62], with different antigen specificities [42,43], so there may be genetically homogeneous subsets of cells. While in principle, we can neglect this heterogeneity in favour of a mean activation rate given that the latent reservoir is large in most PLWH, perhaps depletion of clones with higher activation rates, e.g. those that recognize common antigen, changes the average activation time in a manner that is significant over longer timescales.

These observations motivate investigation of time-inhomogeneous recrudescence rates that decay in time. The modelling attempt in the previous section supports this choice: in comparing figure 3*a*,*b*, we note that the recrudescence rate decreased in order to accommodate long-term viral rebounds. For simplicity, we investigate exponentially decaying recrudescence rates, both single- and biphasic decay. We are guided in our choice by the exponential decay, on average, of the latent reservoir size [52,53]. As the time-dependent recrudescence rate $r(t) = (1 - q(t))a(t)L(t)$, the source of the time-inhomogeneity may be in the activation rate, the probability that a latent cell activation leads to rebound, and the latent reservoir size. Thus, more generally, the probability of viral rebound is given by

$$P_{\mathrm{VR}}(t) = \begin{cases} 0, & 0 \le t < \tau \\ 1 - \exp\left(-\int_\tau^t r(s)\,\mathrm{d}s\right), & t \ge \tau. \end{cases} \tag{3.1}$$

The results of fitting this model to the data are summarized in table 2. First, across all models, the delay τ is remarkably consistent, on the order of 4–5 days (cf. tables 1 and 2, and electronic supplementary material table S1). Further, the data are best explained by the recrudescence rate model (2) in table 2, where the recrudescence rate decays exponentially over time to a constant, non-zero rate. Figure 4 shows that recrudescence rate model (2) effectively recapitulates both the short- and long-term viral dynamics simultaneously not only better than previous models, but very well. We will use this model in our discussion of clinical trial design that follows.

However, note that the estimated delay τ, the initial recrudescence rate r_0, and the initial decay k are the same for recrudescence models (2) and (3), and that the increased ΔAIC of model (3) relative to model (2) results from the difference in the number of parameters (table 2). Moreover, there is significant uncertainty—over many orders of magnitude—in the second phase decay rate. A biphasic recrudescence rate model that decays to a constant (not shown) shows the same trends. From these observations, we conclude that while the recrudescence rate model (2), with uniphasic decay to a constant rate, is the most parsimonious model with the data we have, a repeat of this analysis with more data on post-ATI rebound times may yield a best model with a multi-phasic recrudescence decay rate.

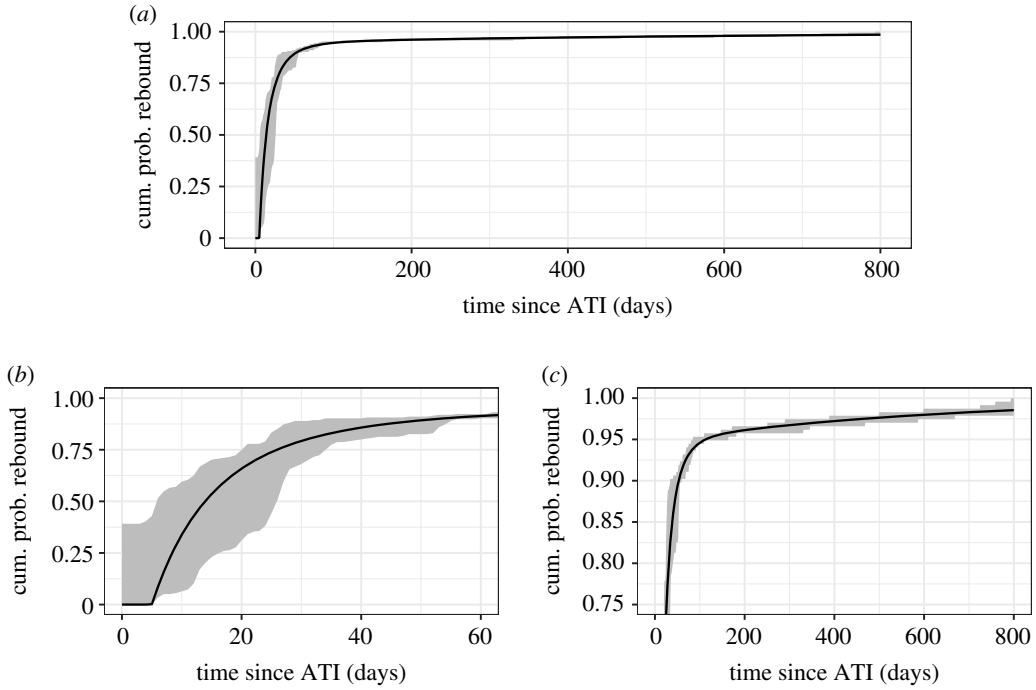

Figure 4. Cumulative probability of viral rebound assuming a single-phase exponentially decaying recrudescence rate model (model (2), see table 2), (*a*) over all time since ATI, (*b*) horizontally zoomed in to early times, to show quality of fit to early-rebound data, and (*c*) vertically zoomed in to highlight the quality of the fit to late-rebound data, not captured by the standard survival distributions tested (figure 2) The shaded region bounds the empirical distributions for the times of last undetectable and first detectable viral load tests across all study participants.

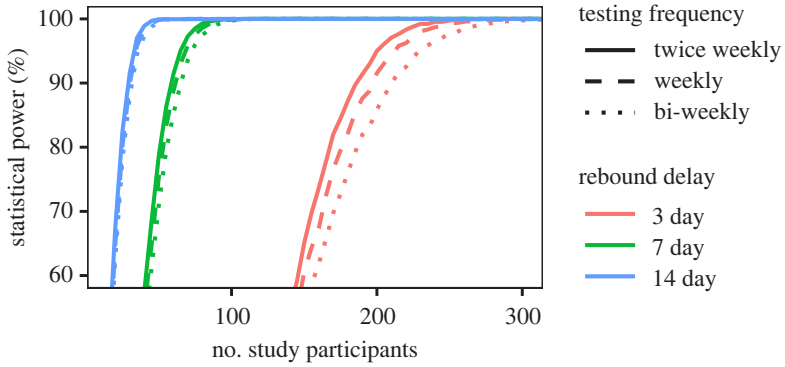

Figure 5. Statistical power of a study to detect a therapy-induced viral rebound delay depending on the number of trial participants, assuming a 3-, 7- or 14-day delay in median time to viral rebound, computed over 10 000 simulated clinical trials lasting 60 days (curves in red, green and blue, respectively), see electronic supplementary material, section A.2 for calculation details. Here we focus on detecting the difference in median rebound time. The line type indicates the assumed testing frequency: twice weekly (solid), weekly (dashed), bi-weekly (dotted). The delay here is generated by assuming that there is an intervention that reduces the constant hazard ratio (HR) from HR = 1 to HR $\approx$ 0.8 (3 day delay); HR $\approx$ 0.6 (1 week delay) and HR $\approx$ 0.4 (2 week delay).

3.4. Application: clinical trial design

The improvement in how well our single-phase exponentially decaying recrudescence rate model explains the data relative to standard survival analysis distributions as well as the constant recrudescence rate model, and goodness of fit, are clear (see figure 4 and tables 1 and 2). We therefore envision an important application of our results to be ATI clinical trial design. Our model provides an analytic form and parameter estimates for the time to viral rebound in the absence of any intervention. Here we offer a key example application, predicting the number of study participants required to detect a viral rebound delay with some desired statistical power.

The role the recrudescence rate plays in our model of viral rebound is that of the hazard function, i.e. the rate that rebound happens at time t, given that it has not yet occurred. Thus, we have shown that the hazard rate

$$h(t) \equiv r(t) = r_\infty + (r_0 - r_\infty)\, \mathrm{e}^{-k(t-\tau)}$$

best explains the current data (table 2). Incidentally, this is why the Gompertz–Makeham distribution [63] was excluded among our stylized distributions (figure 2): its associated hazard rate has the same functional form but is exponentially increasing, rather than decreasing.

Figure 5 illustrates the type of useful predictions that we envision with our model. It shows the statistical significance of a 60-day study depending on the number of ATI study participants required to detect an increased delay following ATI, computed over 10 000 *in silico* trials, see electronic supplementary material, section A.2 for calculation details.

For the purposes of this illustration, we assumed an equal number of participants in the intervention and placebo arms, but in general that need not be the case. We predict, for example, that to detect an intervention-derived 3-day delay in viral rebound with 90% statistical power, our model predicts that would require 210 study participants if testing was performed every two weeks. With a higher frequency of testing, say twice weekly, one would requires fewer study participants—186—to achieve the same statistical power. The number of study participants required to achieve the same power is also decreased if the intervention has greater effect: our model predicts that one would require 59 or 65 study participants, given twice-weekly or bi-weekly testing, respectively, to detect an intervention-induced delay of 7 days with 90% statistical power. For these estimates, we use our time-dependent recrudescence model, which explains the data and therefore provide the most reliable results. And even over a 60-day simulated trial, the more approximate models, e.g. the constant recrudescence model fit only to viral rebound occurring on or before day 60 (figure 3*a*), or the best-fit distribution from survival analysis, the log-logistic (figure 2), yield noticeable under- or overestimates, respectively, for study participants required to achieve some statistical power (see electronic supplementary material, figure S1). Thus, the accuracy provided by our refined model can provide a meaningful correction to simpler models used in clinical trial design.

Note that the above calculation focuses on detecting if rebound time samples are drawn from different distributions, and not on resolving the rebound-time distributions; for that, the number of required study participants would be higher. For this illustration, to create a delay *in silico* we effectively decreased the hazard ratio (HR),

$$\mathrm{HR} = \frac{\text{hazard with intervention}}{\text{hazard without intervention}}.$$

That is, we set the hazard with intervention, $\tilde{h}(t)$, to be the scalar multiple HR of our estimated hazard function $h(t)$, i.e. $\tilde{h}(t) = \mathrm{HR}\,h(t)$. We then used a nonlinear solver to compute HR so that the median time to rebound associated with $\tilde{h}(t)$ is delayed by 3, 7 and 14 days relative to the median time to rebound associated with $h(t)$. Thus, a constant HR of approximately 0.8, 0.6 and 0.4, yield median 3, 7 and 14 day delays, respectively. However, with good support for the biological hypotheses underlying our modelling, we can make similar predictions for interventions that target specific rebound mechanisms. For example, broadly neutralizing antibody interventions that improve immune control [64] would reduce q, the probability that latent cell activation induces rebound (cf. figure 1; recall that the recrudescence rate $r(t) = a(t)L(t)(1 - q(t))$).

4. Discussion

In this study, we developed a model that captures the distribution of times to both short- and long-term HIV viral rebound after therapy interruption and demonstrated its applicability to clinical trial design.

Our model predictions improve significantly upon standard survival models (cf. figures 2 and 4) by considering the underlying biology. Specifically, we rely on the common assumption that HIV viral rebound following treatment suspension is triggered by activation of latently infected cells [28,33–35,39]. While the assumption that recrudescence resulting from such activation occurs at a constant rate explains observations of short-term viral rebound (less than or equal to 60 days) [35,39], it does not explain long-term observations (figure 3). This failure is likely due to the high level of heterogeneity in the latent reservoir. This heterogeneity comes from a variety of sources. The cells in the reservoir each carry a HIV provirus that potentially has a unique ability to reactivate due to a combination of factors including its genetic sequence, the effects of its integration site in the host cell genome [65] as well as epigenetic modifications and the host cell phenotype, e.g. whether it is a central memory, effector memory or transitional memory cell [66]. Each of these cell subtypes have distinct transcriptional and epigenetic programmes that could influence the activity of the integrated HIV promoter. Additionally, biological noise and stochastic fluctuations in transcriptional activity could play an important role in the reversal of latency [67,68]. Lastly, a large fraction of the reservoir is made up of T-cell clones with different antigen specificity [42,43], leading to the possibility that clones with specificity for more common antigens get activated more frequently than clones with specificity for rare antigens. Thus, to the extent that antigen drives proliferation and activation of cells in the reservoir, the reservoir composition could evolve from containing a majority of memory cells to common antigens to a reservoir containing a majority of cells with specificity for rare infrequently encountered antigens [69]. Also, because some are in a deeper state of latency than other cells, possibly due to their integration site [65], the analogous argument could be made that cells in a less deep state of latency activate first successively leaving cells with deeper and deeper latency in the reservoir. Either of these scenarios would be consistent with our finding that the recrudescent rate declines with time, and biologically would be due to a combination of a decline in the per cell activation rate $a(t)$ and in the size of the reservoir $L(t)$. We found that a single-phase decay to a low, constant viral load best explained the data (figure 4 and table 2, model (2)). However, the decay rate was more than an order of magnitude larger than the observed rate of decline of the latent reservoir [52,53] (table 2), consistent with the notion that the activation rate is also decreasing.

We predict an initial average recrudescence frequency of once every 9.4–13.7 days (95% CI for $1/r_0$), which is less frequent than predictions from Pinkevych *et al.* [35]. But this result is not necessarily inconsistent: the difference is only a few days, and our prediction reflects an average over all study participants regardless of drug regimen. Li *et al.* showed in this same cohort a statistically significant delay in rebound in study participants whose ART regimen included NNRTIs (99/235 individuals), which we plan to investigate in a separate study. After several months, the frequency slows down to once every approximately 260–1400 days (approx. 95% CI for $1/r_\infty$). Thus, our modelling suggests that we can roughly consider the latent reservoir as composed of two major populations: cells that activate frequently and deplete rapidly, and cells that activate infrequently. The latter cell population may also include cells in which proviral sequences were integrated further away from transcriptional start sites, thereby producing less virus on average following activation, or possess other structural correlates of viral control [44].

The uncertainty in the late-stage recrudescence rate or frequency reflects the paucity of long-term rebounders in this dataset (cf. table 2). Indeed, we showed that models with more refined decay profiles, e.g. biphasic, yielded the same likelihood as our best-fit uniphasic model, and were judged worse

only because the additional parameters did not provide a better description of the data (cf. table 2). Further, our model, as well as others, assumes that the source of rebound is the latent reservoir [28,33–36,39], which in the presence of ART shows an average, slow decay [52,53]. Following ATI but before viral rebound, it is reasonable to say that the reservoir continues to decay since re-seeding can only be very limited [29], and therefore over long enough times the reservoir should be eliminated. Thus, ultimately we would expect the recrudescence rate to drop to zero. Therefore we anticipate, with the availability of more data, that a more refined decay profile may best explain the data, potentially reflecting sequential depletion of clonal populations of latently infected cells [42,43].

As noted above with regards to drug regimen, in this study we neglected potentially important covariates. Li *et al.* noticed that time of treatment relative to exposure, and pre-ATI ART regimen, both had statistically significant impact on time-to-rebound [12]. With regards to the ART regimen, inclusion of non-nucleoside reverse transcriptase inhibitors (NNRTIs) was associated with longer delays. Also, unsurprisingly, treatment during acute HIV was associated with longer rebound delays than treatment during chronic infection, for which one explanation is a necessarily smaller reservoir [12]. But intriguingly, early treatment initiation—defined in [12] as within six months of exposure to HIV—was associated with still longer rebound delays, pointing to adaptive immune responses as an important actor too. A model accounting for these covariates may yield better prediction and useful biological insights.

We anticipate that the most significant contribution of this study is to ATI clinical trial design since our model offers a marked improvement over survival and other models in terms of explaining the observed distribution of times to viral rebound. Different therapeutic strategies to extend or prevent viral rebound are under investigation (e.g. at the time of this writing, clinical trials include [70–77]). By uniting short- and long-term viral rebound into a single model, well-validated by data (figure 4), we provide an analytic form and parameter estimates for the time to viral rebound in the absence of any intervention. We demonstrated the utility of our model in a power analysis to predict the number of study participants required to detect short intervention-associated delays in viral rebound relative to baseline, depending on the planned testing frequency (figure 5). Our model is mechanistically motivated and considers dynamics of viral rebound. Thus, we can make predictions for interventions that target specific aspects influencing viral rebound. For example, in our recrudescence rate $r(t) = a(t)L(t)(1 - q(t))$, q reflects the probability that latent cell activation leads to rebound, as opposed to the engendered viral lineage going extinct (figure 1). Thus, one could extend our analysis and directly model how antibody interventions improve immune control [64,78] and lead to reductions in q, yielding more realistic analyses.

Ethics. Written informed consent was provided by all study participants for the use of stored samples in HIV-related research. This study was approved by the Pennsylvania State University Institutional Review Board (no. STUDY00004021), the Los Alamos National Laboratory Institutional Review Board (no. LANL 12-02 E), and the Partners Institutional Review Board (no. 2014P000661).

Data accessibility. The data underlying the results in this study are human; ethical and legal restrictions therefore apply. The data are available from the AIDS Clinical Trials Group (ACTG) based on their standard policies. Specifically, the data used in this analysis are publicly available by sending an email to the Statistical and Data Analysis Core of the ACTG (sdac.data@sdac.harvard.edu). See https://actgnetwork.org/clinical-trials/access-published-data for additional details.

Authors' contributions. J.M.C. conceptualized the project, developed and analysed the model, performed related statistical analyses, and drafted and critically revised the manuscript, and acquired project funding; P.M. participated in the modelling analysis; J.Z.L. acquired funding, obtained and curated the data, and critically revised the manuscript; A.S.P. acquired funding and critically revised the manuscript. All authors gave final approval for publication and agree to be held accountable for the work performed therein.

Competing interests. We declare we have no competing interests.

Funding. J.M.C. acknowledges the support of the National Science Foundation (grant no. DMS-1714654) and National Institutes of Health (grant nos. R21-AI143443-01A1 and R01-OD011095). P.M. acknowledges the support of the Penn State Applied Math REU 2018. J.Z.L. acknowledges support by National Institutes of Health (grant nos. AI150396, UM1 AI068636) (AIDS Clinical Trials Group), and a subcontract from UM1 AI068636 to the Harvard Virology Support Laboratory. A.S.P. acknowledges the support of National Institutes of Health (grant nos. R01-AI028433, R01-OD011095, R01-AI152703 and P01-AI131365); his work was performed under the auspices of US Department of Energy (contract 89233218CNA000001).

Acknowledgements. We thank Timothy Charles Reluga for valuable technical discussions and insights. We thank the participants, staff, and principal investigators of the ACTG studies A371 (Paul Volberding, Elizabeth Connick), A5024 (J. Michael Kilby, Ronald Mitsuyasu), A5068 (Jeffrey Jacobson, Ian Frank, Michael Saag, Joseph Eron), A5170 (Daniel Skiest, David Margolis, Diane Havlir) and A5197 (Robert Schooley, Michael Lederman, Diane Havlir). We also thank the efforts of the ACTG NWCS 371 study team.

References

1. Burgoyne R, Tan D. 2008 Prolongation and quality of life for HIV-infected adults treated with highly active antiretroviral therapy (HAART): a balancing act. *J. Antimicrob. Chemother.* **61**, 469–473. (doi:10.1093/jac/dkm499)
2. Beard J, Feeley F, Rosen S. 2009 Economic and quality of life outcomes of antiretroviral therapy for HIV/AIDS in developing countries: a systematic literature review. *AIDS Care* **21**, 1343–1356. (doi:10.1080/09540120902889926)
3. Davey Jr RT *et al.* 1999 HIV-1 and T cell dynamics after interruption of highly active antiretroviral therapy (HAART) in patients with a history of sustained viral suppression. *Proc. Natl Acad. Sci. USA* **96**, 15 109–15 114. (doi:10.1073/pnas.96.26.15109)
4. Sáez-Cirión A *et al.* 2013 Post-treatment HIV-1 controllers with a long-term virological remission after the interruption of early initiated antiretroviral therapy ANRS VISCONTI study. *PLoS Pathog.* **9**, e1003211. (doi:10.1371/journal.ppat.1003211)
5. Lambotte O, Boufassa F, Madec Y, Nguyen A, Goujard C, Meyer L, Rouzioux C, Venet A, Delfraissy JF. 2005 HIV controllers: a homogeneous group of HIV-1-infected patients with spontaneous control of viral replication. *Clin. Infect. Dis.* **41**, 1053–1056. (doi:10.1086/433188)
6. Blankson JN. 2010 Effector mechanisms in HIV-1 infected elite controllers: highly active immune response? *Antivir. Res.* **85**, 295–302. (doi:10.1016/j.antiviral.2009.08.007)
7. Namazi G *et al.* 2018 The control of HIV after antiretroviral medication pause (CHAMP) study: post-treatment controllers identified from 14 clinical studies. *J. Infect. Dis.* **218**, 1954–1963. (doi:10.1093/infdis/jiy479)
8. Sharaf R *et al.* 2018 HIV-1 proviral landscapes distinguish post-treatment controllers from non-controllers. *J. Clin. Invest.* **128**, 4074–4085. (doi:10.1172/JCI120549)
9. Li JZ, Smith DM, Mellors JW. 2015 The critical roles of treatment interruption studies and biomarker

identification in the search for an HIV cure. *AIDS* **29**, 1429–1432. (doi:10.1097/QAD.0000000000000658)

10. Rokx C, Vella S, Pantaleo G, Lévy Y, Boucher CAB. 2016 Unite forces to validate biomarkers in the quest for lasting HIV remission. *AIDS* **30**, 1859–1860. (doi:10.1097/QAD.0000000000001118)
11. Williams JP *et al.* 2014 HIV-1 DNA predicts disease progression and post-treatment virological control. *eLife* **3**, e03821. (doi:10.7554/eLife.03821)
12. Li JZ *et al.* 2016 The size of the expressed HIV reservoir predicts timing of viral rebound after treatment interruption. *AIDS* **30**, 343–353. (doi:10.1097/QAD.0000000000000953)
13. Etemad B *et al.* 2016 Viral and immune characteristics of HIV post-treatment controllers in ACTG studies. In *Conference on Retroviruses and Opportunistic Infections (CROI), 22-25 February, Boston, MA*, abstract 347. See https://www.croiconference.org/abstract/viral-and-immune-characteristics-hiv-post-treatment-controllers-actg-studies/.
14. Martin GE *et al.* 2017 Post-treatment control or treated controllers? Viral remission in treated and untreated primary HIV infection. *AIDS* **31**, 477–484. (doi:10.1097/QAD.0000000000001382)
15. Hurst J *et al.* 2015 Immunological biomarkers predict HIV-1 viral rebound after treatment interruption. *Nat. Commun.* **6**, 8495. (doi:10.1038/ncomms9495)
16. Deeks SG *et al.* 2016 International AIDS Society global scientific strategy: towards an HIV cure 2016. *Nat. Med.* **22**, 839–850. (doi:10.1038/nm.4108)
17. Chun TW, Eisinger RW, Fauci AS. 2019 Durable control of HIV infection in the absence of antiretroviral therapy: opportunities and obstacles. *JAMA* **322**, 27–28. (doi:10.1001/jama.2019.5397)
18. McBrien JB *et al.* 2020 Robust and persistent reactivation of SIV and HIV by N-803 and depletion of CD8+ cells. *Nature* **578**, 154–158. (doi:10.1038/s41586-020-1946-0)
19. Nixon CC *et al.* 2020 Systemic HIV and SIV latency reversal via non-canonical NF-κB signalling *in vivo*. *Nature* **578**, 160–165. (doi:10.1038/s41586-020-1951-3)
20. Perelson AS, Neumann AD, Markowitz M, Leonard JM, Ho DD. 1996 HIV-1 dynamics *in vivo*: virion clearance rate, infected cell life-span, and viral generation time. *Science* **271**, 1582–1586. (doi:10.1126/science.271.5255.1582)
21. Perelson AS, Essunger P, Cao Y, Vesanen M, Hurley A, Saksela K, Markowitz M, Ho DD. 1997 Decay characteristics of HIV-1 infected compartments during combination therapy. *Nature* **387**, 188–191. (doi:10.1038/387188a0)
22. Perelson AS, Nelson PW. 1999 Mathematical analysis of HIV-I: dynamics *in vivo*. *SIAM Rev.* **41**, 3–44. (doi:10.1137/S0036144598335107)
23. Stafford MA, Corey L, Cao Y, Daar ES, Ho DD, Perelson AS. 2000 Modeling plasma virus concentration during primary HIV infection. *J. Theor. Biol.* **203**, 285–301. (doi:10.1006/jtbi.2000.1076)
24. Nowak MA, May R. 2001 *Virus dynamics: mathematical principles of immunology and virology*. Oxford, UK: Oxford University Press.
25. Perelson AS, Ribeiro RM. 2013 Modeling the within-host dynamics of HIV infection. *BMC Biol.* **11**, 96. (doi:10.1186/1741-7007-11-96)
26. Conway JM, Coombs D. 2011 A stochastic model of latently infected cell reactivation a stochastic model of latently infected cell reactivation and viral blip generation in treated HIV patients. *PLoS Comput. Biol.* **7**, e1002033. (doi:10.1371/journal.pcbi.1002033)
27. Conway JM, Konrad BP, Coombs D. 2013 Stochastic analysis of pre- and postexposure prophylaxis against HIV infection. *SIAM J. Appl. Math.* **73**, 904–928. (doi:10.1137/120876800)
28. Conway JM, Perelson AS. 2015 Post-treatment control of HIV infection. *Proc. Natl Acad. Sci. USA* **112**, 5467–5472. (doi:10.1073/pnas.1419162112)
29. Conway JM, Perelson AS. 2016 Residual viremia in treated HIV+ individuals. *PLoS Comput. Biol.* **12**, e1004677. (doi:10.1371/journal.pcbi.1004677)
30. Markowitz M, Louie M, Hurley A, Sun E, Di Mascio M. 2003 A novel antiviral intervention results in more accurate assessment of human immunodeficiency virus type 1 replication dynamics and T-cell decay *in vivo*. *J. Virol.* **77**, 5037–5038. (doi:10.1128/JVI.77.8.5037-5038.2003)
31. Ramratnam B, Bonhoeffer S, Binley J, Hurley A, Zhang LQ. 1999 Rapid production and clearance of HIV-1 and hepatitis C virus assessed by large volume plasma apheresis. *Lancet Infect. Dis.* **354**, 1782–1785. (doi:10.1016/s0140-6736(99)02035-8)
32. Chen HY, Di Mascio M, Perelson AS, Ho DD, Zhang L. 2007 Determination of virus burst size *in vivo* using a single-cycle SIV in rhesus macaques. *Proc. Natl Acad. Sci. USA* **104**, 19 079–19 085. (doi:10.1073/pnas.0707449104)
33. Hill AL, Rosenbloom DIS, Fu F, Nowak MA, Siliciano RF. 2014 Predicting the outcomes of treatment to eradicate the latent reservoir for HIV-1. *Proc. Natl Acad. Sci. USA* **111**, 13 475–13 480. (doi:10.1073/pnas.1406663111)
34. Hill AL, Rosenbloom DIS, Goldstein E, Hanhauser E, Kuritzkes DR, Siliciano RF, Henrich TJ. 2016 Real-time predictions of reservoir size and rebound time during antiretroviral therapy interruption trials for HIV. *PLoS Pathog.* **12**, e1005535. (doi:10.1371/journal.ppat.1005535)
35. Pinkevych M *et al.* 2015 HIV reactivation from latency after treatment interruption occurs on average every 5–8 days—implications for HIV remission. *PLoS Pathog.* **11**, e1005000. (doi:10.1371/journal.ppat.1005000)
36. Pinkevych M *et al.* 2016 Modeling of experimental data supports HIV reactivation from latency after treatment interruption on average once every 5–8 days. *PLoS Pathog.* **12**, e1005740. (doi:10.1371/journal.ppat.1005740)
37. Fennessey CM *et al.* 2017 Genetically-barcoded SIV facilitates enumeration of rebound variants and estimation of reactivation rates in nonhuman primates following interruption of suppressive antiretroviral therapy. *PLoS Pathog.* **13**, e1006359. (doi:10.1371/journal.ppat.1006359)
38. Sneller MC *et al.* 2017 A randomized controlled safety/efficacy trial of therapeutic vaccination in HIV-infected individuals who initiated antiretroviral therapy early in infection. *Sci. Transl. Med.* **9**, eaan8848. (doi:10.1126/scitranslmed.aan8848)
39. Conway JM, Perelson AS, Li JZ. 2019 Predictions of time to HIV viral rebound following ART suspension that incorporate personal biomarkers. *PLoS Comput. Biol.* **15**, e1007229. (doi:10.1371/journal.pcbi.1007229)
40. Bing A, Hu Y, Prague M, Hill AL, Li JZ, Bosch RJ, DeGruttola V, Wang R. 2020 Comparison of empirical and dynamic models for HIV viral load rebound after treatment interruption. *Stat. Commun. Infect. Dis.* **12**, 20190021. (doi:10.1515/scid-2019-0021)
41. Wu Y, Pinkevych M, Xu Z, Keele BF, Davenport MP, Cromer D. 2020 Impact of fluctuation in frequency of human immunodeficiency virus/simian immunodeficiency virus reactivation during antiretroviral therapy interruption. *Proc. R. Soc. B* **287**, 20200354. (doi:10.1098/rspb.2020.0354)
42. Mendoza P, Jackson JR, Oliveira TY, Gaebler C, Ramos V, Caskey M, Jankovic M, Nussenzweig MC, Cohn LB. 2020 Antigen-responsive CD4+ T cell clones contribute to the HIV-1 latent reservoir. *J. Exp. Med.* **217**, e20200051. (doi:10.1084/jem.20200051)
43. Cohn LB, Chomont N, Deeks SG. 2020 The biology of the HIV-1 latent reservoir and implications for cure strategies. *Cell Host Microbe* **27**, 519–530. (doi:10.1016/j.chom.2020.03.014)
44. Jiang C *et al.* 2020 Distinct viral reservoirs in individuals with spontaneous control of HIV-1. *Nature* **585**, 261–267. (doi:10.1038/s41586-020-2651-8)
45. Hill AL, Rosenbloom DIS, Siliciano JD, Siliciano RF. 2016 Insufficient evidence for rare activation of latent HIV in the absence of reservoir-reducing interventions. *PLoS Pathog.* **12**, e1005679. (doi:10.1371/journal.ppat.1005679)
46. Volberding P *et al.* 2009 Antiretroviral therapy in acute and recent HIV infection: a prospective multicenter stratified trial of intentionally interrupted treatment. *AIDS* **23**, 1987–1995. (doi:10.1097/QAD.0b013e32832eb285)
47. Kilby JM *et al.* 2006 A randomized, partially blinded phase 2 trial of antiretroviral therapy, HIV-specific immunizations, and interleukin-2 cycles to promote efficient control of viral replication (ACTG A5024). *J. Infect. Dis.* **194**, 1672–1676. (doi:10.1086/509508)
48. Jacobson JM *et al.* 2006 Evidence that intermittent structured treatment interruption, but not immunization with ALVAC-HIV vCP1452, promotes host control of HIV replication: the results of AIDS clinical trials group 5068. *J. Infect. Dis.* **194**, 623–632. (doi:10.1086/506364)
49. Skiest DJ *et al.* 2007 Interruption of antiretroviral treatment in HIV-infected patients with preserved immune function is associated with a low rate of

clinical progression: a prospective study by AIDS clinical trials group 5170. *J. Infect. Dis.* **195**, 1426–1436. (doi:10.1086/512681)

50. Rosenberg ES *et al.* 2010 Safety and immunogenicity of therapeutic DNA vaccination in individuals treated with antiretroviral therapy during acute/early HIV-1 infection. *PLoS ONE* **5**, e10555. (doi:10.1371/journal.pone.0010555)
51. Schooley RT *et al.* 2010 AIDS clinical trials group 5197: a placebo-controlled trial of immunization of HIV-1-infected persons with a replication-deficient adenovirus type 5 vaccine expressing the HIV-1 core protein. *J. Infect. Dis.* **202**, 705–716. (doi:10.1086/655468)
52. Crooks AM *et al.* 2015 Precise quantitation of the latent HIV-1 reservoir: implications for eradication strategies. *J. Infect. Dis.* **212**, 1361–1365. (doi:10.1093/infdis/jiv218)
53. Siliciano JD, Siliciano RF. 2014 Recent developments in the search for a cure for HIV-1 infection: targeting the latent reservoir for HIV-1. *J. Allergy Clin. Immunol.* **134**, 12–19. (doi:10.1016/j.jaci.2014.05.026)
54. Burnham KP, Anderson DR. 2003 *Model selection and multimodel inference: a practical information-theoretic approach*, 2nd edn. Berlin, Germany: Springer.
55. Luebeck G, Meza R. 2015 *Bhat: general likelihood exploration*. Version 0.9-10. See https://CRAN.R-project.org/package=Bhat.
56. van Dorp CH, Conway JM, Barouch DH, Whitney JB, Perelson AS. 2020 Models of SIV rebound after treatment interruption that involve multiple reactivation events. *Plos Comput. Biol.* **16**, e1008241. (doi:10.1371/journal.pcbi.1008241)
57. Chun TW *et al.* 2010 Rebound of plasma viremia following cessation of antiretroviral therapy despite profoundly low levels of HIV reservoir: implications for eradication. *AIDS* **24**, 2803–2808. (doi:10.1097/QAD.0b013e328340a239)
58. Pannus P *et al.* 2020 Rapid viral rebound after analytical treatment interruption in patients with very small HIV reservoir and minimal on-going viral transcription. *J. Int. AIDS Soc.* **23**, e25453. (doi:10.1002/jia2.25453)
59. Chomont N *et al.* 2009 HIV reservoir size and persistence are driven by T cell survival and homeostatic proliferation. *Nat. Med.* **15**, 893–901. (doi:10.1038/nm.1972)
60. Kearney MF, Wiegand A, Shao W, Coffin JM, Mellors JW, Lederman M, Gandhi RT, Keele BF, Li JZ. 2016 Origin of rebound plasma HIV includes cells with identical proviruses that are transcriptionally active before stopping of antiretroviral therapy. *J. Virol.* **90**, 1369–1376. (doi:10.1128/JVI.02139-15)
61. Simonetti FR *et al.* 2016 Clonally expanded CD4+ T cells can produce infectious HIV-1 *in vivo*. *Proc. Natl Acad. Sci. USA* **113**, 1883–1888. (doi:10.1073/pnas.1522675113)
62. Maldarelli F *et al.* 2014 HIV latency. Specific HIV integration sites are linked to clonal expansion and persistence of infected cells. *Science* **345**, 179–183. (doi:10.1126/science.1254194)
63. Marshall AW, Olkin I. 2007 *Life distributions: structure of nonparametric, semiparametric, and parametric families*. Berlin, Germany: Springer.
64. Nishimura Y *et al.* 2017 Early antibody therapy can induce long-lasting immunity to SHIV. *Science* **543**, 559–563.
65. Einkauf KB *et al.* 2019 Intact HIV-1 proviruses accumulate at distinct chromosomal positions during prolonged antiretroviral therapy. *J. Clin. Invest.* **129**, 988–998. (doi:10.1172/JCI124291)
66. Bradley T, Ferrari G, Haynes BF, Margolis DM, Browne EP. 2018 Single-cell analysis of quiescent HIV infection reveals host transcriptional profiles that regulate proviral latency. *Cell Rep.* **25**, 105–117. (doi:10.1016/j.celrep.2018.09.020)
67. Dar RD, Hosmane NN, Arkin MR, Siliciano RF, Weinberger LS. 2014 Screening for noise in gene expression identifies drug synergies. *Science* **344**, 1392–1396. (doi:10.1126/science.1250220)
68. Cao Y, Lei X, Ribeiro RM, Perelson AS, Liang J. 2018 Probabilistic control of HIV latency and transactivation by the Tat gene circuit. *Proc. Natl Acad. Sci. USA* **115**, 12 453–12 458. (doi:10.1073/pnas.1811195115)
69. Strain MC *et al.* 2003 Heterogeneous clearance rates of long-lived lymphocytes infected with HIV: intrinsic stability predicts lifelong persistence. *Proc. Natl Acad. Sci. USA* **100**, 4819–4824. (doi:10.1073/pnas.0736332100)
70. ClinicalTrials.gov. Identifier NCT04385875. Study to assess the safety and durability of viral control beyond 24 weeks of analytical treatment Interruption after the administration of candidate HIV-1 vaccines DNA.HTI, MVA.HTI and ChAdOx1.HTI or placebo in early treated HIV-1 positive individuals (ATI Extension of AELIX-002 Study); 13 May 2020. https://clinicaltrials.gov/ct2/show/NCT04385875 (accessed 14 December 2020).
71. ClinicalTrials.gov. Identifier NCT03147859. Vedolizumab Treatment in Antiretroviral Drug treated chronic HIV infection (HAVARTI); 10 May 2017. https://clinicaltrials.gov/ct2/show/NCT03147859 (accessed 14 December 2020).
72. ClinicalTrials.gov. Identifier NCT04319367. A randomised placebo controlled trial of ART plus dual long-acting HIV-specific broadly neutralising antibodies (bNAbs). (RIO); 24 March 2020. https://clinicaltrials.gov/ct2/show/NCT04319367 (accessed 14 December 2020).
73. ClinicalTrials.gov. Identifier NCT04319367. Combinatorial therapy to induce an HIV remission; 22 April 2020. https://clinicaltrials.gov/ct2/show/NCT04357821 (accessed 14 December 2020).
74. ClinicalTrials.gov. Identifier NCT02269917. Study to evaluate efficacy and safety of darunavir/cobicistat/emtricitabine/tenofovir alafenamide (D/C/F/TAF) regimen versus boosted protease inhibitor (bPI) along with emtricitabine/tenofovir disoproxil dumarate (FTC/TDF) regimen in virologically-suppressed, HIV-1 infected participants; 21 October 2014. https://clinicaltrials.gov/ct2/show/NCT02269917 (accessed 14 December 2020).
75. ClinicalTrials.gov. Identifier NCT03831945. Combination therapy with VRC-HIVMAB060-00-AB (VRC01) and 10-1074 in HIV-infected individuals undergoing sequential treatment interruptions; 6 February 2019. https://clinicaltrials.gov/ct2/show/NCT03831945 (accessed 14 December 2020).
76. ClinicalTrials.gov. Identifier NCT02850016. Romidepsin Plus 3BNC117 Phase 2a study (ROADMAP); 2016 July 29. https://clinicaltrials.gov/ct2/show/NCT02850016 (accessed 14 December 2020).
77. ClinicalTrials.gov. Identifier NCT02140255. Very early intensive treatment of HIV-infected infants to achieve HIV remission; 16 May 2014. https://clinicaltrials.gov/ct2/show/NCT02140255 (accessed 14 December 2020).
78. Desikan R, Raja R, Dixit N. 2020 Early exposure to broadly neutralizing antibodies may trigger a dynamical switch from progressive disease to lasting control of SHIV infection. *PLoS Comput. Biol.* **16**, e1008064. (doi:10.1371/journal.pcbi.1008064)